Negative Differential Resistance in C_{60}-Based Electronic Devices

Xiaohong Zheng,[†,§] Wenchang Lu,[†,‡,*] Tesfaye A. Abtew,[†] Vincent Meunier,[‡,⊥] and Jerry Bernholc[†,‡]

[†]Center for High Performance Simulation and Department of Physics, North Carolina State University, Raleigh, North Carolina 27695-7518, United States, and [‡]Oak Ridge National Laboratory, Bethel Valley Road, Oak Ridge, Tennessee 37831-6367, United States. [§]Current address: Institute of Solid State Physics, Chinese Academy of Sciences, Hefei, Anhui 230031, China. [⊥]Current address: Department of Physics, Rensselaer Polytechnic Institute, Troy, New York, 12180.

ABSTRACT Unlike single-C_{60}-based devices, molecular assemblies based on two or more appropriately connected C_{60} molecules have the potential to exhibit negative differential resistance (NDR). In this work, we evaluate electron transport properties of molecular devices built from two C_{60} molecules connected by an alkane chain, using a nonequilibrium Green function technique implemented within the framework of density functional theory. We find that electronic conduction in these systems is mediated by the lowest unoccupied molecular orbitals (LUMOs) of C_{60}, as in the case of a single-C_{60}-based device. However, as the positions of the LUMOs are pinned to the chemical potentials of their respective electrodes, their relative alignment shifts with applied bias and leads to a NDR at a very low bias. Furthermore, the position and magnitude of the NDR can be tuned by chemical modification of the C_{60} molecules. The role of the attached molecules is to shift the LUMO position and break the symmetry between the forward and reverse currents. The NDR feature can also be controlled by changing the length of the alkane linker. The flexibility and richness of C_{60}-based molecular electronics components point to a potentially promising route for the design of molecular devices and chemical sensors.

KEYWORDS: molecular device · negative differential resistance · quantum transport · C_{60}; nonequilibrium Green functions

The study of electron transport in molecular devices has been one of the foci in condensed matter physics in recent years. It is expected that molecule-based nanoscale devices[1,2] will offer a viable alternative to traditional silicon-based electronic elements, especially at the scale of future integrated electronic circuits, as they decrease to the sub 10 nm regime.[3,4] Many interesting phenomena have been observed in molecular devices, including highly nonlinear $I-V$ characteristics, negative differential resistance (NDR), electrical switching, rectification, *etc*. NDR is characterized by a decreasing current with increasing bias in some specific bias range. As such, it is one of the key ingredients in a number of electronic components, such as the Esaki and resonant tunneling diodes. Interestingly, it has been observed in scanning tunneling microscopy (STM) measurements for many molecular systems.[5−17]

Several mechanisms have been proposed to explain the observed NDR, such as change of the charge state due to charge transfer, and chemical or conformation changes under finite bias.[5,13,18−23] Lu *et al*. studied the transport properties of a Si/organic-molecule/Si junction,[24] where the electrodes consisted of Si, and highlighted an NDR mechanism based on the relative alignment of the band edges and molecular orbitals. Recently, Chen *et al*. proposed a new mechanism based on local orbital symmetry matching between the electrodes and the molecule.[25] In the above-mentioned systems, NDRs depend on changes in coupling between the electrodes and the molecules, or a change of the electronic level of the molecule under finite bias. Furthermore, this type of behavior can typically only be observed at a relatively high bias. Ideally, NDR-based devices should be developed for operation at much lower bias, for example, in the tens of meV range. This would enable low-voltage nanoelectronic components. Remarkably, even for molecules that do not display an NDR behavior, it is possible to assemble several of them into a single device that can demonstrate NDR. We show below that this is the case for devices assembled out of C_{60} molecules, properly modified with organic linkers.

C_{60}, due to its spherical symmetry and structural stability, has been extensively studied as a functional unit of a molecular device.[26−29] Although it is generally accepted that C_{60} has poor conductance due to its large highest occupied molecular orbital−lowest unoccupied molecular orbital (HOMO−LUMO) gap, a single C_{60}-based molecular device was predicted to have a very high zero-bias conductance at the Fermi energy when placed between

*Address correspondence to luw@chips.ncsu.edu.

Received for review August 4, 2010 and accepted November 09, 2010.

Published online November 17, 2010. 10.1021/nn101902r

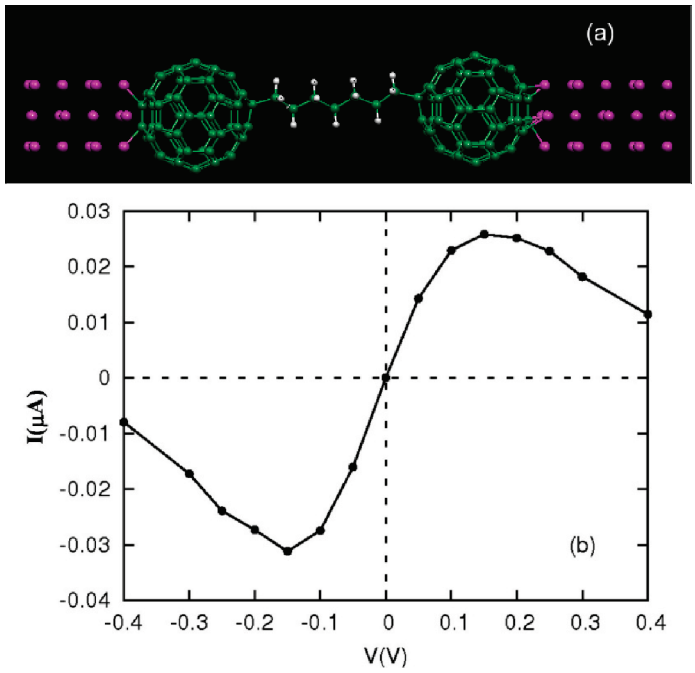

Figure 1. (a) The atomic structure of the $C_{60}-C_7H_{14}-C_{60}$ two-terminal device; red, green, and white spheres represent Al, C, and H atoms, respectively. (b) The calculated $I-V$ curve.

metallic contacts (about $2.2G_0$ when using Au leads, where $G_0 = 2e^2/h$ is the conductance quantum).[26] This high conductance arises from the partially filled LUMOs of the C_{60}, due to charge transfer from the electrodes to the molecule.[26] Furthermore, mechanical deformation of C_{60} by an STM tip can cause a dramatic change to the conductance, as demonstrated by the experimental design of a current amplifier.[27] However, in a single C_{60} device the $I-V$ curve is almost linear in a relatively large bias range,[26] due to a strong coupling between the electrodes and the molecule, as well as broadening of the molecular levels. For this reason, a device based on a single C_{60} coupled to metallic leads does not exhibit NDR.

In this paper, using C_{60} molecules as the basic building blocks, we construct several models of two-terminal devices in which NDR is obtained at very low bias. We point out that our findings do not depend on the type of electrodes used, because the NDR is completely determined by resonant tunneling between the LUMOs of individual C_{60} molecules. Therefore, this kind of a device should be easier to prepare, and the NDR is highly reproducible. In addition, we find that the position of the NDR can be tuned by attaching other appropriate small molecules, which modify the energy level splitting or modulate the distribution of energy levels around the Fermi energy.

RESULTS AND DISCUSSION

The structure of the $C_{60}-C_7H_{14}-C_{60}$ assembly studied here is shown in Figure 1a. It consists of two C_{60} molecules connected by a C_7H_{14} chain and sandwiched between two Al (100) nanowire electrodes. The atomic structure is fully relaxed using DFT total energy calculations. After relaxation, the chemical potential of the right electrode is set to be zero and that of the left electrode is set to the bias voltage. As is well-known, in the single C_{60}-based device, the $I-V$ curve shows a completely symmetrical and almost linear behavior in the low bias range.[26] In contrast, a clear NDR feature appears at a very low bias of 0.15 V for the two-C_{60}s device, with the maximum current of about 30 μA (see Figure 1b). Because of the symmetric geometry, the $I-V$ curve is symmetric for positive and negative biases.

To understand the observed low-bias NDR, it is useful to analyze the evolution of the transmission function as the bias potential is ramped up (see Figure 2). In the equilibrium case, a small charge transfer from the contact to the C_{60} molecule results in a partial occupation of the LUMO state of the C_{60}s. As a result, the transmission is characterized by a main peak around the Fermi level. This peak is due to resonant tunneling between the LUMOs of the two C_{60}s and determines the main features of transport. When a bias is applied, the peak broadens and the current increases, reaching its maximum when the bias is at 0.15 V. When the bias is larger than 0.15 V, the peak height decreases dramatically due to a decreasing overlap between the LUMOs localized on two different C_{60}s. One can see this more clearly from the position-dependent local density of states (LDOS), which are plotted in Figure 3 for the various biases. In the case of zero bias, the levels around the Fermi levels localized on the two C_{60}s are degenerate in energy due to symmetry. The shapes of their wave functions confirm that these are the LUMO levels of the C_{60}s. The main peak in the transmission confirms the tunneling nature of electron transport through

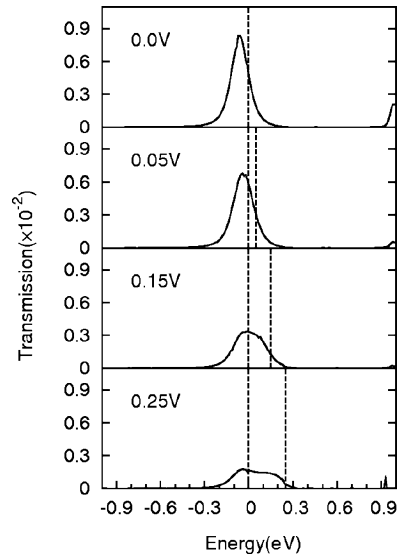

Figure 2. The evolution of the transmission as a function of bias voltage in the $C_{60}-C_7H_{14}-C_{60}$ two-terminal device. The energy zero is at the chemical potential of the right electrode. The two vertical lines indicate the bias window.

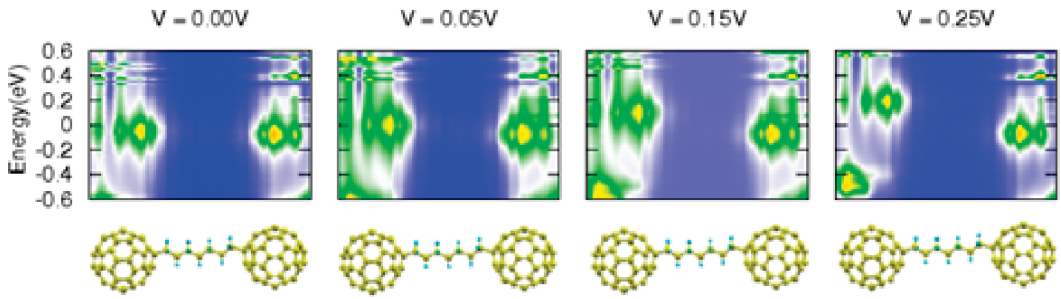

Figure 3. Position-dependent LDOS as a function of bias voltage in the $C_{60}-C_7H_{14}-C_{60}$ two-terminal device. The atomic structures are shown for reference.

these LUMOs, from one C_{60} to the other. This indicates that the electron transport is mediated by LUMOs in this two-C_{60} device, just as in a single-C_{60} device.[26] In real applications, one can also connect the C_{60}s to the electrodes by carbon chains or other molecules, which would result in different charge transfer to/from the C_{60}s. This is an effective way to tune the $I-V$ characteristics.

The reason for the occurrence of NDR at the very small bias of 0.15 V is that resonant tunneling between the two LUMO levels at the two C_{60}s results in a linear increase of current at biases smaller than 0.1 V. However, when the bias is applied, the LUMO levels at each C_{60} follow the chemical potential of the contacted electrode. Therefore, two competing factors affect the final current. One is the integration window, which increases as the bias increases. The other is the overlap between the LUMOs localized at different C_{60}s. As the bias increases, the LUMO levels of the two C_{60}s broaden and shift away from each other. Their overlap in energy becomes small, which results in a broadening of the transmission peak with simultaneous decrease in height (see Figure 2). These two factors give rise to the NDR peaks at $\pm$0.15 V in the $I-V$ curve.

In the above analysis, we find that the only appreciable effect of the bias is to rigidly shift the individual energy levels of the C_{60}s. Furthermore, by analyzing the potential drop in the system, we find that the drop mainly takes place in the alkane chain region; the drop at the interfaces between the electrodes and the C_{60}s being negligible. This shows that the resistances of the interfaces between the electrodes and C_{60}s are much smaller than that of the alkane chain. At a small finite bias, the band structure in each of the electrodes is shifted rigidly, because the bias corresponds to a shift of the chemical potential, and the LUMO of each C_{60} appears pinned to the band structure of its electrode. We can therefore explain the NDR in this device using only the relative shifts of the LUMOs of the C_{60}s and resonant tunneling between them.

The above results indicate that the linker between the two C_{60}s, in our case the alkane chain, plays a crucial role in the development of NDR. To understand the effects of chain length on the transport properties, we consider C_3H_6 and $C_{11}H_{22}$ in addition to C_7H_{14}. As expected, the current decreases exponentially with an increase of the length (see Figure 4a,b). Its dependence on length can be fitted as

$$I = I_0 e^{-\beta L}$$

where I_0 = 76.63 μA and β = 0.72 Å^{-1} at a bias of 0.1 V.[30] Interestingly, the effect of the chain length on the NDR position is very small: while varying the linker from C_3H_6 to $C_{11}H_{22}$, the NDR position changes only by 0.02 V. This can be understood by the fact that the energy position of the NDR is governed by the positions of quasi-molecular orbitals of the C_{60}s, as explained above.

It is important to emphasize that the NDR mechanism described above is different from those previously presented in the literature.[5,13,18−23] It is neither caused by a change of the coupling between the electrodes and the central molecule nor by a chemical or

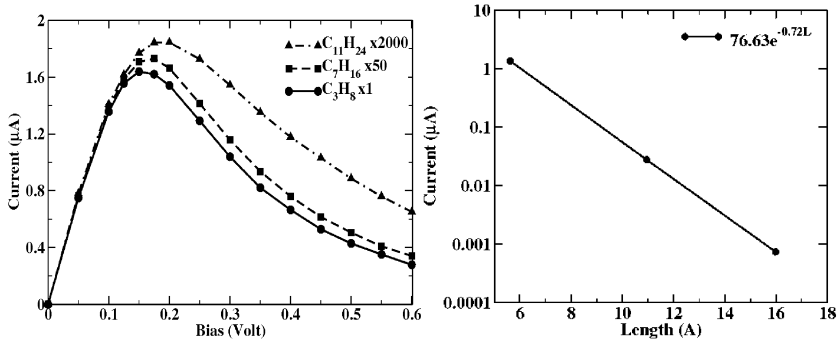

Figure 4. The NDR as a function of the chain length: (a) $I-V$ curves for C_3H_6, C_7H_{14}, and $C_{11}H_{22}$, respectively. Compared to the C_3H_6 case, the currents for C_7H_{14} and $C_{11}H_{22}$ cases are scaled 50- and 2000-fold, respectively. (b) Exponential fit of the current as a function of chain length for bias of 0.1 V.

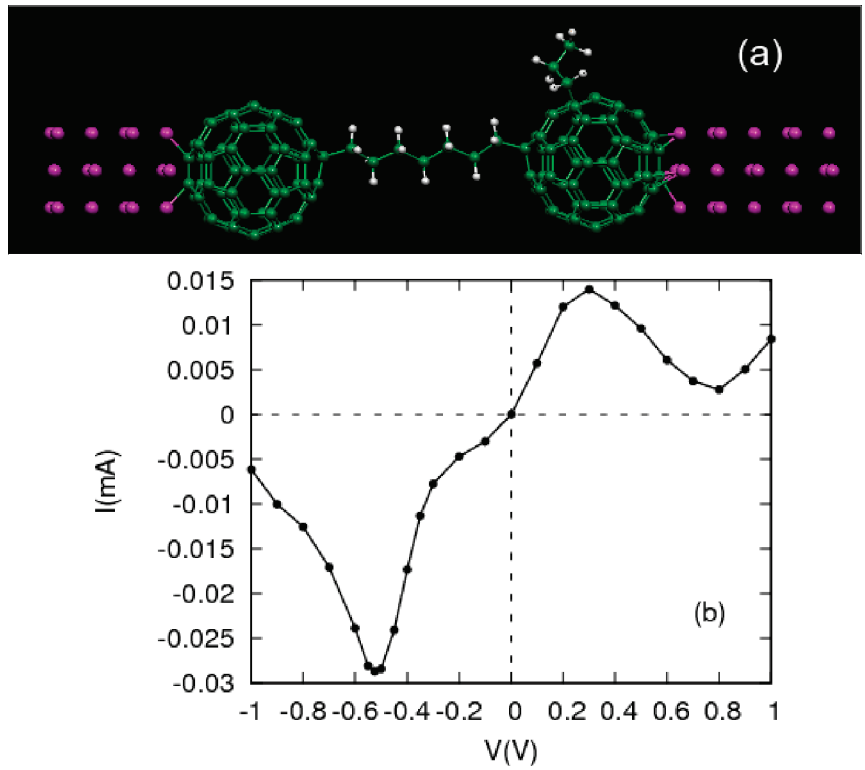

Figure 5. The two-C_{60}-based device with C_3H_7 attached to the right C_{60}. (a) The atomic structure of the system with Al atoms marked in red, C atoms in green, and H atoms in white. (b) The *I*−*V* characteristic.

conformational change of the central molecule under finite bias. Furthermore, it is not caused by a change of the alignment between the levels of the central molecule and the band edges of the electrodes. In our case, the NDR is completely determined by resonant tunneling between two C_{60} molecules connected by a chemical linker that has much larger HOMO−LUMO gap than the C_{60}s and thus acts as a barrier. Therefore, the NDR mechanism studied in this paper is not related to changes in coupling between the electrodes and the conductor, and it should not depend on the type of materials used for the metallic electrodes. In fact, this behavior is very similar to the simple system of two aluminum atoms studied by Lang,[31] where tunneling also resulted in the appearance of a NDR. However, the two-C_{60}-based device is much more complex, flexible, and certainly more chemically inert. Furthermore, the properties of C_{60} can be modulated in many ways, such as doping, molecular adsorption, and mechanical deformation, which would all alter the electron transport properties, while the magnitude of the current can be adjusted by changing the properties of the linker.

Since the NDR here is caused by relative shifts of the LUMO levels of the C_{60}s, its position could be modulated by changing the positions of the LUMO levels by, for example, adsorption of different molecules on the C_{60}. As an example, we consider a small alkane, C_3H_7, adsorbed on one of the C_{60} molecules (see Figure 5a). After the adsorption, the positions of the NDR shift to −0.55 V in the negative bias region with the maximum current of 30 μA, and to 0.30 V in the positive bias region with the maximum current of 15 μA (Figure 5b). The transmission function at equilibrium is mainly characterized by two peaks, one at the Fermi level and one at about −0.50 eV (Figure 6). When the bias is swept in the negative direction, the peak at the Fermi level gradually disappears, since the overlap with the LUMO at the left C_{60} becomes smaller, while the height of the peak at −0.50 eV increases and reaches its maximum when it aligns with the LUMO level of the left C_{60}. This is the reason why the NDR appears at about −0.50 V. When the bias is swept in the positive direction, the peak at the Fermi level shifts to higher energy and its magnitude also changes, while the height of the peak at −0.50 eV decreases.

SUMMARY

We proposed several configurations of two-terminal devices that use C_{60} molecules as the basic building blocks and investigated their transport properties. We found that the electron conduction is mediated by the LUMOs of the C_{60}s, just as in single-C_{60}-based devices. The NDR, present only in the two-C_{60} devices, can be explained by the alignment of LUMO levels of the left and right C_{60}s. At equilibrium, the LUMO levels lie very close to the Fermi level, due to charge transfer from the electrodes to the C_{60}s. As the bias increases, the LUMOs shift with the chemical potential of their respective electrodes and become misaligned, leading to a decrease in the current and thus an NDR. It is important

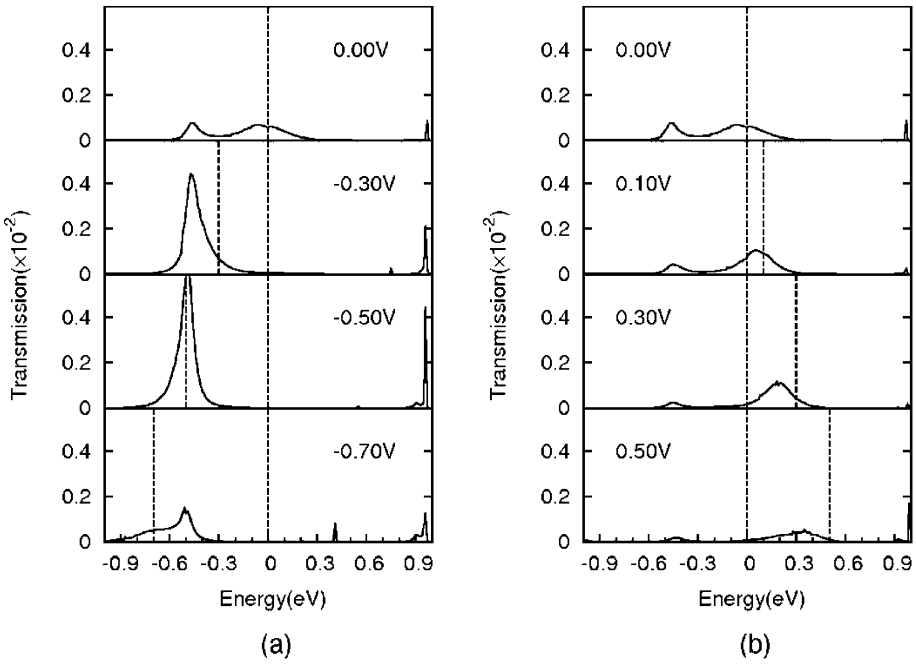

Figure 6. The evolution of the transmission as a function of bias in the two-C_{60} device shown in Figure 5 (a) for negative bias and (b) for positive bias. The chemical potential of the right electrode is set to zero and the two vertical lines indicate the bias window.

to note that the proposed NDR mechanism should not depend on the type of metallic electrodes used, since resistances at the interfaces between the Al electrodes and C_{60} molecules turned out to be negligible compared with that of the alkane chain. It follows that the NDR is completely determined by resonant tunneling between the LUMOs of the C_{60}s. The position of the NDR can be controlled by attaching small molecules or in other ways that affect the relative positions of the left and right LUMOs of the C_{60}s. The possibility of tuning the NDR position and strength provides some design flexibility when devising molecular electronics and could be used to adapt the device to a particular function. Conversely, the sensitivity of the NDR to molecular adsorption could enable its use of C_{60}-based devices in molecular sensing.

ATOMIC STRUCTURE AND COMPUTATIONAL METHODOLOGY

The model structures studied here are constructed as follows: In a two-terminal device, two C_{60} molecules are connected by alkane chains containing $n = 3, 7, 11$ carbon atoms. Two hydrogen atoms at the end of each alkane chain C_nH_{2n+2} are removed to bond with C_{60}s, which results in C_nH_{2n} linkers between the C_{60} molecules. Each C_{60} is directly connected to an aluminum nanowire acting as an electrode. The nanowire has bulk aluminum structure and extends along the (100) direction. It consists of alternating 5- and 4-atom layers in the fcc geometry (Figure 1a). We divide the whole system into three parts: the left electrode, the right electrode, and the "conductor" part. The latter includes the C_{60} molecules connected *via* the alkane chain and four terminating layers of the left and right Al electrodes.

The calculations are carried out using a massively parallel real-space multigrid implementation[32] of density-functional theory (DFT).[33] Both the Al electrodes and the conductor parts are described at the same DFT footing. The exchange and correlation terms are represented by the generalized gradient approximation (GGA) in the Perdew, Burke, and Ernzerhof form.[34] The ions are represented by nonlocal ultrasoft pseudopotentials.[35] The conductance and nonlinear $I-V$ characteristics are studied by the nonequilibrium Green function (NEGF) method[36−39] in a basis of optimally localized orbitals.[40−42] The localized orbitals are centered on each atom and optimized variationally in the equilibrium geometry. We use five orbitals per atom with a cutoff radius of 4.2 Å. The wave functions and localized orbitals are described on a uniform grid with spacing of 0.18 Å. When external bias is applied, the system is out-of-equilibrium and the electronic structure changes depending on the bias. Because the bias greatly affects the transport properties of molecular devices,[24] a fully self-consistent calculation of the electronic structure in the central region is performed at each bias voltage before the transmission coefficient and the current are calculated.

The transmission coefficient is obtained from the Landauer formula

$$T(E, V) = \frac{2e^2}{h} Tr[\Gamma_L(E, V)\, G^R(E)\, \Gamma_R(E, V)\, G^A(E)]$$

where $G^{R,A}$ are the retarded/advanced Green functions of the conductor part and $\Gamma_{L,R}$ are the coupling functions to the left/right electrodes. The current through this system is calculated by integrating the transmission function over the bias window $eV = \mu_L - \mu_R$,

$$I(V) = \int_{-\infty}^{\infty} T(E, V)[f(E - \mu_L) - f(E - \mu_R)]\, dE$$

where f is the Fermi distribution function and $\mu_{L,R}$ is the chemical potentials of the two electrodes.

Acknowledgment. X.Z. was supported by ONR N000140610173, W.L. and J.B. by DOE DE-FG02-98ER45685, T.A. by DOE DE-FG05-08OR23331, and V.M. by DE-AC05-00OR22725.

Note Added after ASAP Publication: This paper published ASAP on November 17, 2010 without the Acknowledgments. The corrected version reposted on December 9, 2010.

REFERENCES AND NOTES

1. Aviram, A.; Ratner, M. A. Molecular Rectifiers. *Chem. Phys. Lett.* **1974**, *29*, 277–283.
2. Reed, M. A.; Zhou, C.; Muller, C. J.; Burgin, T. P.; Tour, J. M. Conductance of a Molecular Junction. *Science* **1997**, *278*, 252–254.
3. Leong, M.; Doris, B.; Kedzierski, J.; Rim, K.; Yang, M. Silicon Device Scaling to the Sub-10-nm Regime. *Science* **2004**, *306*, 2057–2060.
4. International Technology Roadmap for Semiconductors. www.itrs.net.
5. Chen, J.; Reed, M. A.; Rawlett, A. M.; Tour, J. M. Large On−Off Ratios and Negative Differential Resistance in a Molecular Electronic Device. *Science* **1999**, *286*, 1550–1552.
6. Chen, J.; Wang, W.; Reed, M. A.; Rawlett, A. M.; Price, D. W.; Tour, J. M. Room-Temperature Negative Differential Resistance in Nanoscale Molecular Junctions. *Appl. Phys. Lett.* **2000**, *77*, 1224–1226.
7. Gorman, C. B.; Carroll, R. L.; Fuierer, R. R. Negative Differential Resistance in Patterned Electroactive Self-Assembled Monolayers. *Langmuir* **2001**, *17*, 6923–6930.
8. Fan, F. R. F.; Yang, J. P.; Cai, L. T.; Price, D. W.; Dirk, S. M.; Kosynkin, D. V.; Yao, Y. X.; Rawlett, A. M.; Tour, J. M.; Bard, A. J. Charge Transport through Self-Assembled Monolayers of Compounds of Interest in Molecular Electronics. *J. Am. Chem. Soc.* **2002**, *124*, 5550–5560.
9. Amlani, I.; Rawlett, A. M.; Nagahara, L. A.; Tsui, R. K. An Approach to Transport Measurements of Electronic Molecules. *Appl. Phys. Lett.* **2002**, *80*, 2761–2763.
10. Rawlett, A. M.; Hopson, T. J.; Nagahara, L. A.; Tsui, R. K.; Ramachandran, G. K.; Lindsay, S. M. Electrical Measurements of a Dithiolated Electronic Molecule *via* Conducting Atomic Force Microscopy. *Appl. Phys. Lett.* **2002**, *81*, 3043–3045.
11. Le, J. D.; He, Y.; Hoye, T. R.; Mead, C. C.; Kiehl, R. A. Negative Differential Resistance in a Bilayer Molecular Junction. *Appl. Phys. Lett.* **2003**, *83*, 5518–5520.
12. Walzer, K.; Marx, E.; Greenham, N. C.; Less, R. J.; Raithby, P. R.; Stokbro, K. Scanning Tunneling Microscopy of Self-Assembled Phenylene Ethynylene Oligomers on Au(111) Substrates. *J. Am. Chem. Soc.* **2004**, *126*, 1229–1234.
13. Lyo, I. W.; Avouris, P. Negative Differential Resistance on the Atomic Scale—Implications for Atomic Scale Devices. *Science* **1989**, *245*, 1369–1371.
14. Bedrossian, P.; Chen, D. M.; Mortensen, K.; Golovchenko, J. A. Demonstration of the Tunnel−Diode Effect on an Atomic Scale. *Nature* **1989**, *342*, 258–260.
15. Guisinger, N. P.; Greene, M. E.; Basu, R.; Baluch, A. S.; Hersam, M. C. Room Temperature Negative Differential Resistance through Individual Organic Molecules on Silicon Surfaces. *Nano Lett.* **2004**, *4*, 55–59.
16. Grobis, M.; Wachowiak, A.; Yamachika, R.; Crommie, M. F. Tuning Negative Differential Resistance in a Molecular Film. *Appl. Phys. Lett.* **2005**, *86*, 3.
17. Gaudioso, J.; Lauhon, L. J.; Ho, W. Vibrationally Mediated Negative Differential Resistance in a Single Molecule. *Phys. Rev. Lett.* **2000**, *85*, 1918.
18. Seminario, J. M.; Zacarias, A. G.; Tour, J. M. Theoretical Study of a Molecular Resonant Tunneling Diode. *J. Am. Chem. Soc.* **2000**, *122*, 3015–3020.
19. Seminario, J. M.; Zacarias, A. G.; Derosa, P. A. Theoretical Analysis of Complementary Molecular Memory Devices. *J. Phys. Chem. A* **2001**, *105*, 791–795.
20. Seminario, J. M.; Cordova, L. E.; Derosa, P. A. An *ab Initio* Approach to the Calculation of Current−Voltage Characteristics of Programmable Molecular Devices. *Proc. IEEE* **2003**, *91*, 1958–1975.
21. Taylor, J.; Brandbyge, M.; Stokbro, K. Conductance Switching in a Molecular Device: The Role of Side Groups and Intermolecular Interactions. *Phys. Rev. B* **2003**, *68*, 121101.
22. Shi, X. Q.; Zheng, X. H.; Dai, Z. X.; Wang, Y.; Zeng, Z. Changes of Coupling Between the Electrodes and the Molecule under External Bias Bring Negative Differential Resistance. *J. Phys. Chem. B* **2005**, *109*, 3334–3339.
23. He, J.; Lindsay, S. M. On the Mechanism of Negative Differential Resistance in Ferrocenylundecanethiol Self-Assembled Monolayers. *J. Am. Chem. Soc.* **2005**, *127*, 11932–11933.
24. Lu, W. C.; Meunier, V.; Bernholc, J. Nonequilibrium Quantum Transport Properties of Organic Molecules on Silicon. *Phys. Rev. Lett.* **2005**, *95*, 206805.
25. Chen, L.; Hu, Z. P.; Zhao, A. D.; Wang, B.; Luo, Y.; Yang, J. L.; Hou, J. G. Mechanism for Negative Differential Resistance in Molecular Electronic Devices: Local Orbital Symmetry Matching. *Phys. Rev. Lett.* **2007**, *99*, 146803.
26. Taylor, J.; Guo, H.; Wang, J. *Ab Initio* Modeling of Open Systems: Charge Transfer, Electron Conduction, and Molecular Switching of a C_{60} Device. *Phys. Rev. B* **2001**, *63*, 121104.
27. Joachim, C.; Gimzewski, J. K. An Electromechanical Amplifier Using a Single Molecule. *Chem. Phys. Lett.* **1997**, *265*, 353–357.
28. Ono, T.; Hirose, K. First-Principles Study of Electron-Conduction Properties of C_{60} Bridges. *Phys. Rev. Lett.* **2007**, *98*, 026804.
29. Xie, R.-H.; Bryant, G. W.; Zhao, J.; Smith, V. H.; Di Carlo, A.; Pecchia, A. Tailorable Acceptor C_{60}-*n*Bn and Donor C_{60}-*m*Nm Pairs for Molecular Electronics. *Phys. Rev. Lett.* **2003**, *90*, 206602.
30. Kaun, C.-C.; Larade, B.; Guo, H. Electrical Transport Through Oligophenylene Molecules: A First-Principles Study of the Length Dependence. *Phys. Rev. B* **2003**, *67*, 121411.
31. Lang, N. D. Resistance of Atomic Wires. *Phys. Rev. B* **1995**, *52*, 5335.
32. Briggs, E. L.; Sullivan, D. J.; Bernholc, J. Real-Space Multigrid-Based Approach to Large-Scale Electronic Structure Calculations. *Phys. Rev. B* **1996**, *54*, 14362.
33. Kohn, W.; Sham, L. J. Self-Consistent Equations Including Exchange and Correlation Effects. *Phys. Rev.* **1965**, *140*, A1133.
34. Perdew, J. P.; Burke, K.; Ernzerhof, M. Generalized Gradient Approximation Made Simple. *Phys. Rev. Lett.* **1996**, *77*, 3865.
35. Vanderbilt, D. Soft Self-Consistent Pseudopotentials in a Generalized Eigenvalue Formalism. *Phys. Rev. B* **1990**, *41*, 7892.
36. Larade, B.; Taylor, J.; Mehrez, H.; Guo, H. Conductance, *I*−*V* Curves, and Negative Differential Resistance of Carbon Atomic Wires. *Phys. Rev. B* **2001**, *64*, 075420.
37. Taylor, J.; Guo, H.; Wang, J. *Ab Initio* Modeling of Quantum Transport Properties of Molecular Electronic Devices. *Phys. Rev. B* **2001**, *63*, 245407.
38. Brandbyge, M.; Mozos, J.-L.; Ordejón, P.; Taylor, J.; Stokbro, K. Density-Functional Method for Nonequilibrium Electron Transport. *Phys. Rev. B* **2002**, *65*, 165401.
39. Xue, Y. Q.; Datta, S.; Ratner, M. A. First-Principles Based Matrix Green's Function Approach to Molecular Electronic Devices: General Formalism. *Chem. Phys.* **2002**, *281*, 151–170.
40. Fattebert, J. L.; Bernholc, J. Towards Grid-Based O(N) Density-Functional Theory Methods: Optimized Nonorthogonal Orbitals and Multigrid Acceleration. *Phys. Rev. B* **2000**, *62*, 1713.
41. Nardelli, M. B.; Fattebert, J. L.; Bernholc, J. O(N) Real-Space Method for *ab Initio* Quantum Transport Calculations: Application to Carbon Nanotube and Metal Contacts. *Phys. Rev. B* **2001**, *64*, 245423.
42. Wang, S. C.; Lu, W. C.; Zhao, Q. Z.; Bernholc, J. Resonant Coupling and Negative Differential Resistance in Metal/Ferrocenyl Alkanethiolate/STM Structures. *Phys. Rev. B* **2006**, *74*, 195430.